

## **КОРРОЗИОННЫЕ И ТРИБОТЕХНИЧЕСКИЕ СВОЙСТВА Fe – W – Mo, Fe – Co – W И Fe – Cr – Ni СТАЛЕЙ ПОСЛЕ НИЗКОЭНЕРГЕТИЧЕСКОЙ ИОННОЙ БОМБАРДИРОВКИ**

<sup>1</sup>А.Г. Артемчик, <sup>2</sup>А.Л. Жарин, <sup>1</sup>А.Н. Карпович, <sup>1</sup>А.А. Колесникова

<sup>1</sup>Физико-технический институт НАН Беларуси

<sup>2</sup>Белорусский национальный технический университет

г. Минск, Республика Беларусь

*Традиционные методы триботехнических и коррозионных испытаний, наряду с методом работы выхода электрона использованы для изучения влияния ионно-лучевого азотирования на физико-химические свойства Fe – W – Mo, Fe – Co – W и Fe – Cr – Ni сталей. Показано существенное увеличение коррозионной стойкости и снижение коэффициента трения сталей, прошедших ионно-лучевую обработку.*

**Ключевые слова:** Fe – W – Mo, Fe – Co – W и Fe – Cr – Ni стали, ионно-лучевое азотирование, структура, фазовый состав, твердость, коэффициент трения, износостойкость, коррозионная стойкость

## **CORROSION AND TRIBOTECHNICAL PROPERTIES OF Fe – W – Mo, Fe – Co – W and Fe – Cr – Ni STEELS AFTER LOW ENERGY NITROGEN ION BOMBARDMENT**

<sup>1</sup>A.G. Artsemchyk, <sup>2</sup>A.L. Zharin, <sup>1</sup>A.N. Karpovich, <sup>1</sup>A.A. Kolesnikova

<sup>1</sup>Physical-Technical Institute of the National Academy of Sciences of Belarus

Minsk, Republic of Belarus

<sup>2</sup>Belarusian National Technical University,

Minsk, Republic of Belarus

*Traditional techniques of tribological and corrosion tests, as well as recently developed Kelvin probe technique were used to understand nitrogen ion beam influence on physical-chemical properties of Fe – W – Mo, Fe – Co – W and Fe – Cr – Ni steels. Dramatic increase of corrosion resistance and smaller values of coefficient of friction for ion implanted steels was observed.*

**Keywords:** Fe – W – Mo, Fe – Co – W and Fe – Cr – Ni steels, ion-beam nitriding, structure, phase composition, hardness, friction factor, wear resistance, corrosion resistance

**E-mail:** vmo@tut.by

Ion implantation is widely used for surface hardening of the cutting tool. Recently it was demonstrated that low-energy, high-current-density ion implantation improves dramatically the tribological properties of ferrous materials and modifies a comparatively deep surface layer. Data have been presented which show that solid solutions, precipitates of new phases and sometimes amorphization of surface layers with thickness up to several  $\mu\text{m}$  and more are induced by low-energy high-current density ion implantation. The phase formed are controlled by the implantation parameters, which can be maintained easily and precisely to ensure optimum properties of the surface [1–3].

In this research the influence of nitrogen ion implantation on the microstructure of high speed (Fe – W – Mo and Fe – Co – W) and corrosion-resistance (Fe – Cr – Ni) steels has been investigated to ensure the optimum combination of the bulk and surface layer mechanical and chemical properties.

HSS16SX, HSS16DX, 25W20Co20Cr4V2M, 12Cr18Ni10Ti and 55Cr20Mn9AlNi4 steels were selected for analysis in the research. The chemical composition of steel samples was determined using a X-ray fluorescence spectrometer Pioneer S4 (Bruker Corporation). Data of the analysis are presented in Table 1.

Before ion beam processing steel samples were grinded and polished on “Tegramin-30” machine (Struers ApS) to a roughness parameter  $R_a \leq 0,08 \mu\text{m}$ .

Implanter equipped with Hall-type ion source was used for nitrogen ion beam processing. Samples were implanted with 3 keV nitrogen ions at an ion current density (dose rate) of 2 mA/cm<sup>2</sup>. These conditions correspond to an integrated fluence of  $3,9 \times 10^{19} \text{ cm}^{-2}$ .

The temperatures of the steels samples were monitored during implantation using a thermocouple located 2 mm from the surface being treated. Samples were held at 670 K, 720 K, 770 K, or 820 K during implantation. The minimal of these temperatures was selected on the basis of preliminary research [1], which demonstrated that 620 K was sufficient to yield a modified surface layer that was several tenths of a  $\mu\text{m}$  thick. The maximal temperature was selected to avoid solid solution decomposition accompanied by the degradation of mechanical and corrosive properties of steels occur above 770 K.

X-ray diffractometer DRON-3M (monochromatic  $\text{CoK}_\alpha$  irradiation, voltage 30 kV, current 20 mA) was used for microstructure analysis. JCPDS data base and Selyakov-Scherrer method were used to read and analyze diffraction spectra.

Corrosion tests were carried out by gravimetric method and samples were held for 550 hours in 10 % NaCl solution.

Surface hardness was measured at a 0,1 N load with a 10 s dwell time. Ten measurements were made on each sample, so statistically significant mean values could be obtained.

The electron work function (EWF) was measured by Kelvin technique, based on vibrating condenser, which determines contact potential difference (CPD) arising between the indenter and steel sample. Data for CPD were converted to EWF surface distributions [4–6].

Ball on disk wear tests without lubrication were carried out on tribometer JLTB-02 (J&L Tech Co) at normal load 2 N, angle speed 120 r/min, friction path 250 m, ambient temperature 12, 5 °C and humidity 48 %.

Data of X-ray analysis are presented in Table. 2.

The main carbide phase in virgin samples for Fe – Co – W steel was  $(\text{Fe},\text{M})_6\text{C}$  with a complex f.c.c. crystal lattice (spatial group Fd3mp). It was demonstrated elsewhere [7], that saturation of the matrix phase of the steel with nitrogen at sufficiently high temperatures results in formation of nitrogen solid solutions,  $\gamma'$  and  $\epsilon$  nitrides and carbonitride phases  $\text{M}_6(\text{C},\text{N})$  and  $\text{V}(\text{C},\text{N})$  isomorphic to the corresponding carbide phases. It's known,  $\gamma'$ -phase observed in the surface layers of nitride steels demonstrates the best tribological characteristics.

It has been established, that ion-beam treatment of Fe – W – Mo steels at 770 K leads to release a large number of dispersed nitride particles in the surface layers and the micro-

Table 1

## Chemical composition of steel samples before and after nitrogen ion implantation

Steel	Mode of processing	Concentration of elements, weight %									
		C	Cr	Mn	W	Mo	Co	V	Ni	Si	Ti
HSS16SX	Virgin	0,85	3,85	0,31	5,76	4,91	0,17	1,84	0,24	0,30	-
	670 K	0,80	3,9	0,36	5,75	5,2	0,179	1,86	0,24	0,34	-
	770 K	0,86	3,92	0,40	5,72	4,99	0,18	1,89	0,27	0,25	-
HSS16DX	Virgin	0,80	4,27	0,38	18,5	0,73	0,31	1,18	0,45	0,27	-
	670 K	0,78	4,32	0,42	17,9	0,92	0,38	1,23	0,55	0,35	-
	770 K	0,82	4,40	0,45	17,5	0,86	0,45	1,38	0,48	0,44	-
25W20Co20Cr4V2M	Virgin	0,27	3,78	0,20	19,84	0,15	18,68	1,57	0,14	0,15	-
	670 K	0,25	3,78	0,22	19,82	0,16	18,70	1,55	0,14	0,15	-
	770 K	0,26	3,77	0,20	19,84	0,17	18,66	1,58	0,15	0,16	-
12Cr18Ni10Ti	Virgin	0,11	18,51	1,95	-	-	-	-	9,96	0,65	0,66
	670 K	0,12	18,63	1,80	-	-	-	-	9,11	0,71	0,69
	770 K	0,11	17,77	1,83	-	-	-	-	9,13	0,68	0,64
55Cr20Mn9AlNi4	Virgin	0,53	21,43	8,89	-	-	-	-	3,50	0,38	-
	670 K	0,53	21,47	9,02	-	-	-	-	3,55	0,32	-
	770 K	0,52	21,80	9,12	-	-	-	-	3,41	0,30	-

hardness of modified layers reaches to 12 000 MPa. The nitrogen-treated layer includes martensite, austenite,  $\eta$ -W<sub>6</sub>C, carbonitride V (C, N),  $\varepsilon$ -phase and nitride phase  $\gamma'$ -Fe<sub>4</sub>N [8–10].

**Table. 2**

**Depth of modified surface layer, microhardness and phase composition of ion implanted samples**

Steel	Mode of processing	Depth of modified layer, $\mu\text{m}$	Micro-hardness, MPa	Main phases
HSS16SX	Virgin	–	7700	$\alpha$ -Fe, $\gamma$ , $\eta$ -M <sub>6</sub> C, VC
	670 K	12	10800	$\alpha$ -Fe, $\gamma$ , $\eta$ -M <sub>6</sub> C, VC, $\varepsilon$
	770 K	40	11800	$\gamma$ , $\alpha_N$ , $\eta$ -M <sub>6</sub> C, V(C,N), $\gamma'$ , $\varepsilon$ , amorphous phase
HSS16DX	Virgin	–	8450	$\alpha$ -Fe, $\eta$ -M <sub>6</sub> C, VC
	670 K	10	15600	$\alpha$ -Fe, $\eta$ -M <sub>6</sub> C, VC, $\alpha_N$
	770 K	40	20000	$\alpha_N$ , $\eta$ -M <sub>6</sub> C, VC, $\varepsilon$
25W20Co20Cr4V2M	Virgin	–	5300	$\alpha$ -Fe, $\eta$ -M <sub>6</sub> C, $\theta$ -Co <sub>7</sub> W <sub>6</sub>
	670 K	10	11200	$\alpha_N$ , $\alpha''$ -(Fe,Co) <sub>8</sub> N
	770 K	45	12300	$\alpha_N$ , $\alpha''$ -(Fe, Co) <sub>8</sub> N, Co <sub>2</sub> N
12Cr18Ni10Ti	Virgin	–	2500	$\gamma$ -Fe
	670 K	3–5	10000	$\gamma$ -Fe, $\gamma'_N$
	770 K	17–20	15000	CrN, $\alpha$ -Fe, $\gamma'_N$
55Cr20Mn9AlNi4	Virgin	–	3500	$\gamma$ -Fe, M <sub>23</sub> C <sub>6</sub>
	670 K	6–8	7000	$\gamma$ -Fe, $\gamma'_N$ , CrN, $\alpha$ -Fe
	770 K	15–25	14500	$\gamma'_N$ , CrN, $\alpha$ -Fe

As for corrosion-resistance (Fe – Cr – Ni) steels, ion-beam treatment at 670 K and above leads to the release of a large number CrN and ferromagnetic particles  $\alpha$ -Fe. A significant increase in the concentration of nano-sized CrN and  $\alpha$ -Fe particles is observed after treatment at a temperature above 720 K. As a result of the transformation of the austenite, a large amount of CrN and  $\alpha$ -phase and decrease of concentration of the  $\gamma$ -phase are recorded [11].

The results of corrosion tests (Fig. 1) in 10 % aqueous NaCl solution demonstrated effectiveness of ion-beam processing essentially at the initial period of tests (around 100 hours). Gradual dissolution of the surface layer results in significant increase of corrosion rate.

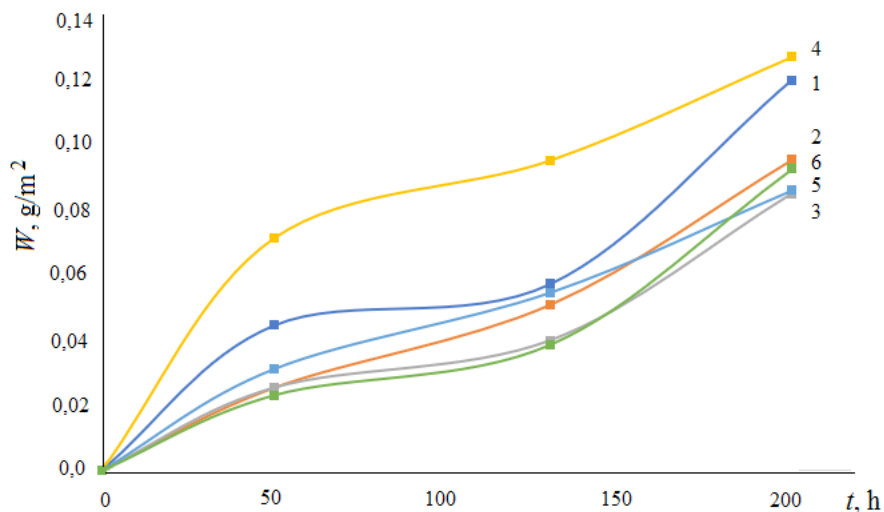


Fig. 1. Dependences mass wearing ( $W$ ,  $\text{g}/\text{m}^2$ ) of steels processed in different modes in 10 % aqueous NaCl solution:

1 – virgin HSS16SX steel; 2 – HSS16SX steel ion beam implanted at 670 K; 3 – 770 K;  
4 – virgin 55Cr20Mn9AlNi4 steel; 5 – 55Cr20Mn9AlNi4 ion beam implanted at 670 K; 6 – at 770 K

The structural-phase state of the surface layers of the studied materials has a significant effect on the dissolution rate in 10 % aqueous NaCl solution (Fig. 2).

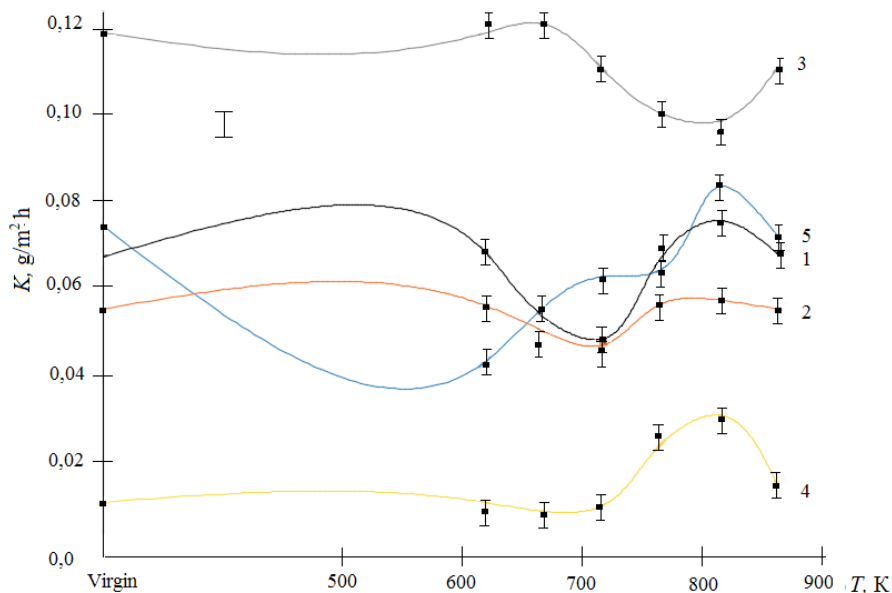


Fig. 2. Corrosion rate ( $K$ ,  $\text{g}/\text{m}^2\cdot\text{h}$ ) in 10 % aqueous solution of NaCl of analyzed steels processed with nitrogen ions at various temperatures:

1 – HSS16SX; 2 – HSS16DX; 3 – 25W20Co20Cr4V2M; 4 – 12Cr18Ni10Ti4; 5 – 55Cr20Mn9AlNi4

As for corrosion tests of 25W20Co20Cr4V2M steel, it was found the highest corrosion resistance is achieved at the stages where special nitrides precipitate. They bind V and W atoms to form the nitride VN and  $W_2N$  particles (Fig. 2,1). The rate of steel corrosion falls by  $\approx 20\%$ . The formation of the special VN and  $W_2N$  nitrides and the decomposition of nitrogen martensite after high temperature nitriding of the steel at 820 K lead to the restoration of its corrosion resistance to the level of the initial

quenched state. A possible reason for increased corrosion resistance of the layers containing VN and W<sub>2</sub>N nitrides is a decrease in electrochemical activity of vanadium and tungsten atoms as a result of their binding into chemically resistant mononitride interstitial phases with a cubic lattice [7].

Corrosion resistance of 12Cr18Ni10Ti steel after ion treatment at 670 K is close to that for virgin steel (Fig. 2,4). Increasing the temperature to 770 K leads to a sharp deterioration in corrosion properties. This is explained by significant changes in the phase composition (see Table. 2). For steel 55Cr20Mn9AlNi4 ion treatment at 620–720 K leads to an increase in corrosion resistance of approximately 2–2,5 times (Fig. 2,5). This is due to the formation of corrosion-resistant phases and a homogeneous modified layer thickness of 10–15 μm. The increase in the corrosion rate at high processing temperatures is due to the intensive destruction of chromium-depleted austenite after the dissolution of the modified layer. The increased content of Cr and Mn in 55Cr20Mn9AlNi4 steel improves resistance to corrosion at high treatment temperatures [11].

Fig. 3 shows surface distribution of CPD for analyzed steels steel samples. The distributions of CPD values demonstrate inhomogeneity of virgin and ion implanted surface microstructures.

Increasing of the treatment temperature to 770 K leads to a significant decrease of the values of CPD in comparison with the virgin state (from (–18)–0 to (–40)–(–30) mV) for high-speed steels and from 25–35 to ((–25)–(–14) mV) for Cr–Ni steels). A further temperature increase leads to growing in the values of the CPD to the values of virgin steel. In addition, the surface of the samples after ion-beam treatment have a more uniform distribution of the CPD [12].

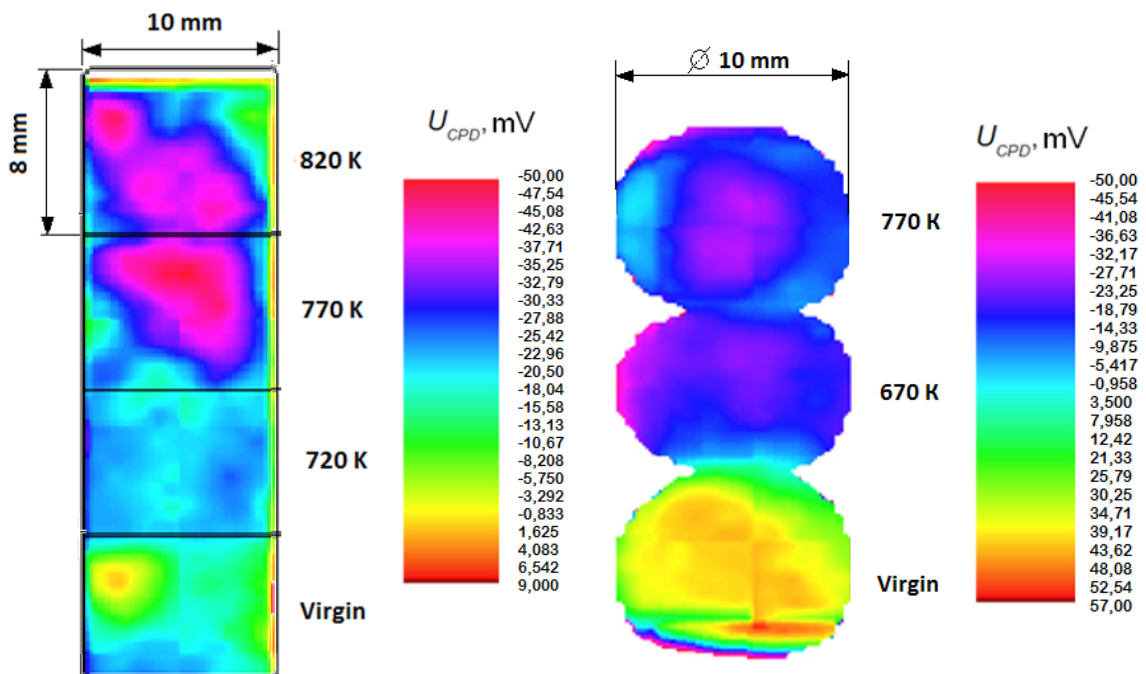


Fig. 3. Surface distribution of CPD of HSS16DX (1) and 12Ch18Ni10T (2) steel blocks versus temperature of ion-beam processing

Thus, it is established that the treatment at temperatures up to 720–770 K leads to an increase of EWF (table 3), distributed on the surface of steels, which is consistent with the data on the determination of corrosion resistance (Fig. 3, 2).

**Table. 3**

**The values of EWF distributed on the surface of ion implanted samples**

Mode of processing	The values of EWF, meV			
	HSS16SX	HSS16DX	12Cr18Ni10Ti	55Cr20Mn9AlNi4
Virgin	22	25	-42	-56
620	25	30	-30	-40
670	30	34	13	-35
720	48	38	30	56
770	32	56	25	24
820	32	46	-35	-43
870	25	32	-40	-52

The increase of EWF of the investigated samples treated with nitrogen ions to 770 K is explained by the increase in the electron concentration of metal atoms saturated with nitrogen. Particularly, electron density increase results in EWF growth. Most of ion implanted nitrogen ions are located in interstitial pores of matrix crystal lattice [12–13]. Nitrogen atoms located in octahedral pores lose their  $p$ -electrons from outer  $1s^2 2s^2 p^3$  shell. As a consequence, electron concentration and EWF increase. Processing temperature increase results in higher diffusivity of nitrogen atoms. Spatial distribution of implanted atoms becomes more homogeneous. Simultaneously nitrogen atoms interact with chromium and form nanosized CrN inclusions. More homogeneous distribution and depleting of solid solution with nitrogen results in EWF decrease after high temperature processing.

Corrosion processes were more intense in areas with a maximum values of CPD (R 1,2 mm) and on areas with a large gradient of CPD values (R 2,8 mm) (see fig. 3,1). The samples with uniform distribution of the CPD on the surface corroded with the same intensity (fig. 3.2).

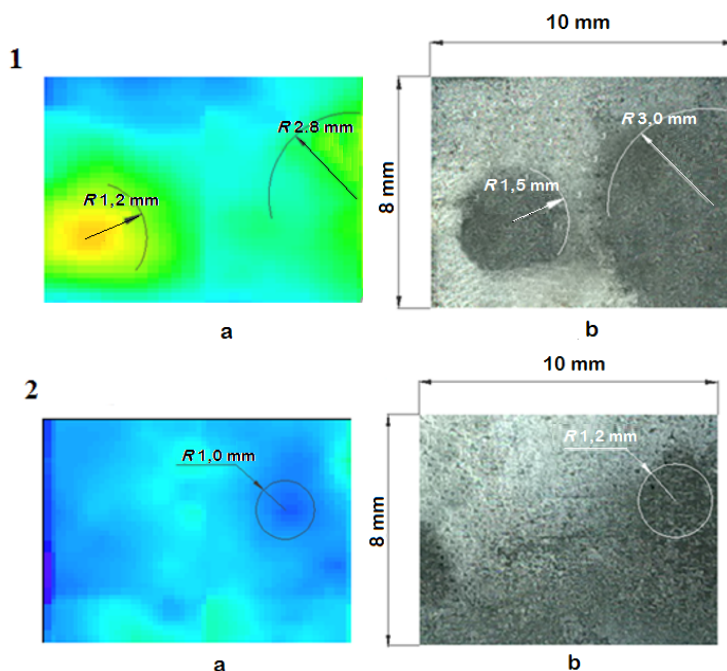


Fig. 4. The distribution of the CPD values on the surface of the specimens of high speed steel prior to corrosion tests (a) and after corrosion tests (550 h in NaCl) (b):  
1 – virgin steel; 2 – HSS16DX steel ion beam implanted at 720 K

Thus, the pattern of surface corrosion destruction of studied materials and pattern of the distribution of the CPD are same. Therefore, the monitoring of EWF is effective method of control conditions and properties of surface layers of materials.

Fig. 5 shows the dependences of mass wear on the sliding path of the 25W20Co20Cr4V2M (a) and 12Cr18Ni10Ti (b) steels treated under different temperature modes [7, 11].

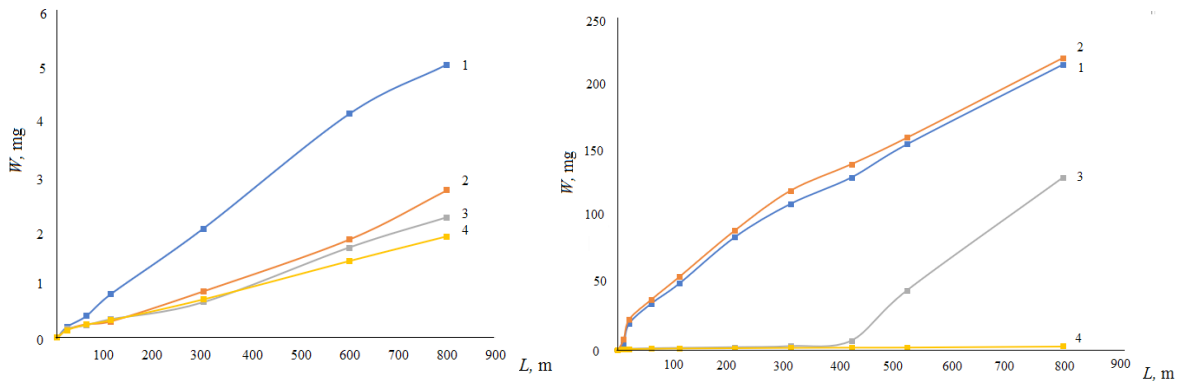


Fig. 5 – Dependences of the mass wearing of 25W20Co20Cr4V2M (a) and 12Cr18Ni10Ti (b) steels processed in different modes:

1 – virgin steel; 2 – steel ion beam implanted at 670 K; 3 – at 720 K; 4 – at 770 K

Results of tribological tests are presented in Fig. 6. P6M5 and P18 steel samples demonstrated practically the same coefficient of friction. Ion beam processing of samples resulted in friction coefficient decrease from 0,55–0,6 to 0,4–0,45. The most dramatic variation of friction coefficient took place during running-in period.

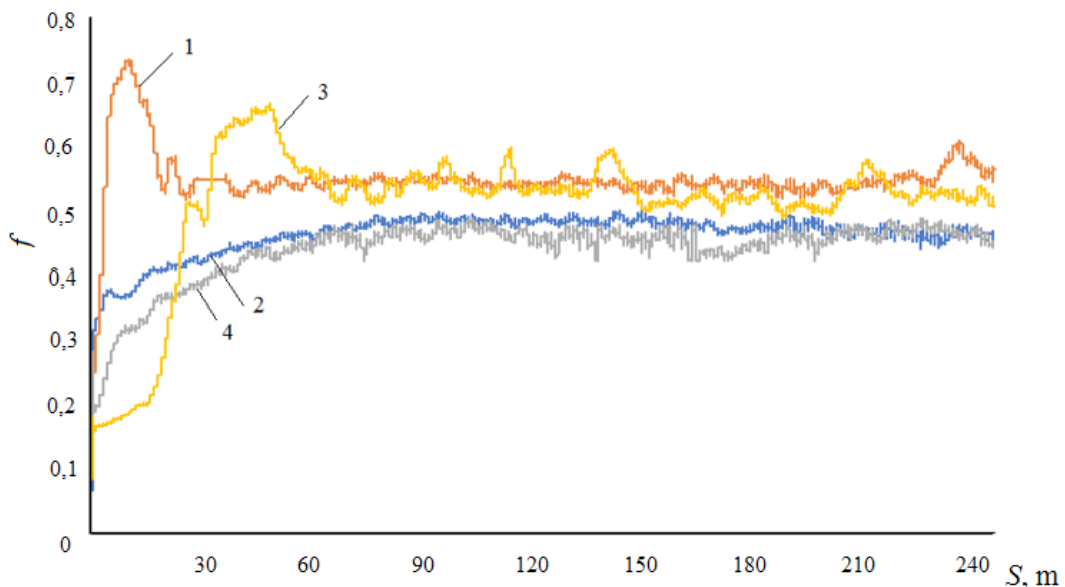


Fig. 6. Coefficient of friction versus friction path:

1 – virgin P6M5 steel; 2 – P6M5 steel ion beam implanted at 770 K;  
3 – virgin P18 steel; 4 – P18 steel ion beam implanted at 770 K

The table lists the data on the intensity of wearing and the friction coefficient of the surface layers of the steel implanted with nitrogen ions (see table 4).



**Table. 4****Intensity of wearing and friction coefficient of modified surface layers**

Steel	Mode of processing	Intensity of wearing, $\text{lg}\cdot 10^{-3} \text{ mg/m}$	Friction coefficient, $f$
HSS16SX	Virgin	2,08	0,55–0,6
	670 K	1,17	0,50–0,55
	720 K	2,5	0,40–0,45
	770 K	2,5	0,40–0,45
25W20Co20Cr4V2M	Virgin	5,7	0,70–0,90
	670 K	3,6	0,90–1,0
	720 K	2,81	0,85–0,90
	770 K	2,66	0,80–0,90
12Cr18Ni10Ti	Virgin	268,8	0,82–0,85
	670 K	275,0	0,80–0,90
	720 K	162,5	0,75–0,80
	770 K	3,75	0,60–0,65

It is obvious that the ion-beam treatment leads to a significant increase in wear resistance of the surface steels layers. In particular, the intensity wearing of high speed steel after ion processing under 770 K decreases by 1,5–2,0 times. Besides, the wear resistance of chrome nickel steel increases by 30 times. The friction coefficient of the steel after nitrogen ion modification lowers from 0,6 to 0,4 for Fe – W – Mo steel, from 0,9 to 0,8 for Fe – Co – W steel and from 0,85 to 0,60 for Fe – Cr – Ni steel).

**Conclusions**

1. High-current-density nitrogen ion beam processing effectively influences surface microstructure, mechanical and corrosion properties of high speed steels. It is shown that saturation of the surface steel layers with nitrogen ions leads to an increase in microhardness to 12 GPa for Fe – Co – W steel, to 15 GPa for Fe – Cr – Ni steel and 20 GPa for Fe–W–Mo steel.

2. Well-defined correlation between electron work function and corrosion resistance of high speed steels has been established. It was demonstrated that corrosion processes are more intense in areas with a maximum values of CPD and on areas with a large gradient of CPD values.

3. It was demonstrated that corrosion rate decreases at a factor of 3–4 as a consequence of nitrogen ion beam processing for high speed steels and at a factor of 2–2,5 for Fe – Cr – Ni steels.

4. Coefficient of dry friction for investigated steels after ion beam processing decreases at 20–30 % and wear resistance increases by a factor of 2 compared with the initial state for high speed steels and by a factor of 30 corrosion-resistance steels.

**ЛИТЕРАТУРА**

1. Инженерия поверхностей конструкционных материалов с использованием плазменных и пучковых технологий / А.В. Белый [и др.]. – Минск: Беларуская навука, 2017. – С. 456.
2. Wilbur, P.J. Engineering Tribological Surfaces by Ion Implantation / P.J. Wilbur, B.W. Buchholtz. // Surface Coating Technology. – 1996. Vol. 79. – P. 8 – 21.
3. Ozturk, O. Microstructural, Mechanical, and Corrosion Characterization of Nitrogen Implanted Plastic Injection Mould Steel / O. Ozturk // Surface and Coatings Technology. 2005. – V. 196. P. 333–340.
4. Zharin, A.L. Application of Macro and Micro Kelvin Probe in Tribological Studies / A.L. Zharin // Fundamentals of Tribology and Bridging the Gap Between Macro and Micro Nanoscales. – Netherlands: Kluwer Academic Publishers, 2001. P. 445 – 466.

5. Yamamoto, S. Work function of binary compounds / S. Yamamoto, K. Susa, U. Kawabe. – Japan J. Appl. Phys. 2,1974. P. 209–215.
6. Работа выхода электрона и физико-механические свойства хромсодержащих ионно-легированных сталей / А.В. Белый [и др.] // Весці нацыянальнай акадэміі навук Беларусі, 2016. №1. С. 21–27.
7. Byeli, A.V. Choi Structure and Properties of Tool Maraging Fe – Co – W Steel / A.V. Byeli, V.A. Kukareko, K.I. Choi // Processed with Concentrated Flows of Nitrogen Ions. Inorganic Materials: Applied Research, 2012, Vol. 3, No. 4, pp. 309–313.
8. Effect of Ion-Bram Nitriding on Structure, Phase State, and Tribological Behavior of Efficient Thermal Spray Costings Deposited from Various Classes of Rod Steels / V.A. Kukareko [et al.] // Journal of Friction and Wear. – 2013. – Vol. 34. P. 475 – 480.
9. Byeli, A.V. Aspects of the Formation of a Nitrogen-Modified Layer upon the Ion-Beam Treatment of Hypersonic Thermal Spray Coating of Austenitic Steel Journal of Surface Investigation X-ray, Synchrotron and Neutron Techniques / A.V. Byeli, A. N. Grigorchik, V. A. Kukareko. – 2016, Vol. 10, P. 712–717.
10. Ионно-лучевое азотирование вольфрамсодержащей быстрорежущей стали: структурно-фазовые превращения и свойства / А.Н. Карпович [и др.] // Современные методы и технологии создания материалов: международная научная конференция, Минск, 14–16 сентября, 2016 / Физико-технический институт национальной академии наук Беларуси; под ред. С.А. Астапчика [и др.]. – 2016. – Т. 2. – С. 145–149.
11. Karpovich, A.N. Ion beam processing of austenite steels: Tribotechnical and corrosion properties / A.N. Karpovich, A.V. Byeli, V.A. Kukareko // J. Frict. Wear. – November 2016, Volume 37, Issue 6. – P. 519–522.
12. Byeli, A.V. Titanium and zirconium based alloys modified by intensive plastic deformation and nitrogen ion implantation for biomedical implants / A.V. Byeli, V.A. Kukareko, A.G. Kononov // Journal of the Mechanical behavior of Biomedical Materials. Vol. 6.2012. P. 89–94.

## REFERENCES

1. Byeli A.V., Kalinichenko A.S., Devoyno O.G., Kukareko V.A. Inzheneriya poverhnostej konstrukcionnyh materialov s ispol'zovaniem plazmennyh i puchkovykh tekhnologij [Surface Engineering of Construction Materials by Plasma and Beam Technologies]. Minsk: Belaruskaya Navuka, 2017. 456 p. (in Russian)
2. Wilbur P.J., Buchholtz B.W. Engineering Tribological Surfaces by Ion Implantation / Surface Coating Technology. – 1996. Vol. 79. – P. 8 – 21.
3. Ozturk O. Microstructural, Mechanical, and Corrosion Characterization of Nitrogen Implanted Plastic Injection Mould Steel //Surface and Coatings Technology. 2005. – V. 196. P. 333–340.
4. Zharin A.L. Application of Macro and Micro Kelvin Probe in Tribological Studies // Fundamentals of Tribology and Bridging the Gap Between Macro and Micro Nanoscales. – Netherlands: Kluwer Academic Publishers, 2001. P. 445 – 466.
5. Yamamoto S., Susa K., Kawabe U. Work function of binary compounds, Japan J. Appl. Phys. 2,1974. P. 209–215.
6. Byeli A.V., Karpovich A.N., Zharin A.L., Tiavlovskij A.K. Rabota vyhoda ehlektrona i fiziko-mekhanicheskie svojstva hromsoderzhashchih ionno-legirovannyh stalej [Electron work function and physical-mechanical properties of chromium-containing ion-doped steels] / Proceedings of the National Academy of Sciences of Belarus, 2016. №1. P. 21–27. (in Russian)
7. Byeli A.V., Kukareko V.A., Choi K.I. Structure and Properties of Tool Maraging Fe – Co – W Steel / Processed with Concentrated Flows of Nitrogen Ions. Inorganic Materials: Applied Research, 2012, Vol. 3, No. 4, pp. 309–313.
8. Kukareko V.A., Byeli A.V., Belotserkovskii M.A. and Grigorchik A.N. Effect of Ion-Bram Nitriding on Structure, Phase State, and Tribological Behavior of Efficient Thermal Spray Costings Deposited from Various Classes of Rod Steels. Journal of Friction and Wear. – 2013. – Vol. 34. P. 475 – 480.
9. Byeli A.V., Grigorchik A. N., Kukareko V. A. Aspects of the Formation of a Nitrogen-Modified Layer upon the Ion-Beam Treatment of Hypersonic Thermal Spray Coating of Austenitic Steel Journal of Surface Investigation X-ray, Synchrotron and Neutron Techniques // 2016, Vol. 10, P. 712–717.
10. Karpovich A.N., Byeli A.V., Grishkevich A.A., Kolecnikova A.A. Ionno-luchevoe azotirovanie vol'framsoderzhashchej bystrorezhushchej stali: strukturno-fazovye prevrashcheniya i svojstva [Ion-beam nitriding of tungsten-containing high-speed steel: structural-phase transformations and properties] / Advanced methods and technologies of materials development and processing: International Scientific and Technical Conference, Minsk, September 14–16, 2016 / The Physical-technical Institute of the National Academy of Sciences of Belarus; edited by S.A. Astapchic [and others.]. – 2016. – Vol. 2. – P. 145–149. (in Russian)
11. Karpovich A.N., Byeli A.V., Kukareko V.A. Ion beam processing of austenite steels: Tribotechnical and corrosion properties / J. Frict. Wear. – November 2016, Volume 37, Issue 6. – P. 519–522.
12. Byeli A.V., Karpovich A.N., Zharin A.L., Tiavlovskij A.K. Electron work function and physical-mechanical properties of chromium-containing ion-doped steels / Proceedings of the National Academy of Sciences of Belarus, 2016. №1. P. 21–27. (in Russian)
13. Byeli A.V., Kukareko V.A., Kononov A.G. Titanium and zirconium based alloys modified by intensive plastic deformation and nitrogen ion implantation for biomedical implants / Journal of the Mechanical behavior of Biomedical Materials. Vol. 6.2012. P. 89–94.

*Статья поступила в редакцию в окончательном варианте 21.06.18*